

## Investigation and Simulation of Catalytic Reforming Reactions of Iraqi Heavy Naphtha Using Pt-Sn/Al<sub>2</sub>O<sub>3</sub> and Pt-Ir/Al<sub>2</sub>O<sub>3</sub> Catalysts

**Dr. Khalid A. Sukkar**

Petroleum Technology Department, University of Technology /Baghdad  
Email: khalid\_ajmee@yahoo.com

**Dr. Shahrazad R. Raouf,** 

Chemical Engineering Department, University of Technology/Baghdad

**Dr. Ramzy S. Hamied,** 

Petroleum Technology Department, University of Technology / Baghdad

Received on: 30/9/2012 & Accepted on: 7/3/2013

### ABSTRACT

In the present work experimental and simulation studies have been carried out to describe the reaction kinetics of catalytic reforming process using Iraqi heavy naphtha as a feedstock. Two types of bi-metals catalysts were prepared (Pt-Sn/Al<sub>2</sub>O<sub>3</sub> and Pt-Ir/Al<sub>2</sub>O<sub>3</sub>) supported on  $\gamma$ -Al<sub>2</sub>O<sub>3</sub>.

The main three described reforming reactions were investigated (dehydrogenation, dehydrocyclization, and hydrocracking) to characterize catalysts performance in term of activity and selectivity. The performances of catalysts were investigated under the following operating conditions: reaction temperature range of 480-510 °C, weight hour space velocity range of 1-2 hr<sup>-1</sup>, pressure at 6 atm, and hydrogen to hydrocarbon ratio of 4:1.

The results showed that the higher conversion of Iraqi heavy naphtha components (i.e., paraffins and naphthenes) increased with temperature whereas, weight hourly space velocity has shown inverse impact on conversion. On the other hand, it was concluded that the yields of aromatics and high components are increased for both types of catalysts (Pt-Sn/Al<sub>2</sub>O<sub>3</sub> and Pt-Ir/Al<sub>2</sub>O<sub>3</sub>) under the same operating conditions.

A comprehensive mathematical model and simulation was developed in the present work to describe the reaction kinetics of reforming reactions. The comparison between the concentration of (paraffin's, naphthenes, and aromatics), and temperature profile of experimental and simulation results showed a good agreement and the deviation confined between them in the range of 1.93% to 14.51%.

**Key words:** Experimental and Simulation; catalytic reforming; Pt-Sn/Al<sub>2</sub>O<sub>3</sub> and Pt-Ir/Al<sub>2</sub>O<sub>3</sub> catalysts.

## دراسة عملية ومحاكاة تفاعلات التهذيب لمادة النفط العراقية الثقيلة باستخدام عوامل مساعدة Pt-Sn/Al<sub>2</sub>O<sub>3</sub> and Pt-Ir/Al<sub>2</sub>O<sub>3</sub> ثنائية المعدن

### الخلاصة

تضمن البحث اعداد دراسة شاملة عملية ونظرية للعوامل المساعدة ثنائية المعدن المحملة على الالومينا (Pt-Sn/Al<sub>2</sub>O<sub>3</sub> Pt-Ir/Al<sub>2</sub>O<sub>3</sub>) المستخدمة في عملية التهذيب باستخدام مادة النفط الثقيلة (العراقية) كمادة اولية للعملية. من اجل دراسة امكانية زيادة كفاءة العملية وتحسين انتقائية العوامل المساعدة تم خلال البحث دراسة التفاعلات الرئيسية التي تحدث في عملية التهذيب وهي ( تفاعلات ازالة الهيدروجين, تفاعلات تكوين المركبات الحلقية وكذلك تفاعلات التكسير الحراري) بوجود الهيدروجين. تم دراسة اداء نوعين من العوامل المساعدة الثنائية المعدن حسب الظروف التشغيلية التالية: السرعة الفراغية للغاز (1-2 ساعة<sup>-1</sup>), درجة حرارة التفاعل تتراوح بين (510-480 م°). أثبتت النتائج العملية ان نسبة التحول لمادة النفط الثقيلة (المواد البرافينية والمواد النفثينية) تزداد مع زيادة درجة حرارة التفاعل وتقل مع زيادة السرعة الفراغية. كذلك لوحظ ان الانتاجية (yield) للمواد العطرية والمركبات الخفيفة تزداد لجميع انواع العوامل المساعدة المحضرة.

تم اعداد دراسة نظرية شاملة تضمنت بناء وتطوير موديل رياضي يصف ديناميكية التفاعل لعملية التهذيب بالعامل المساعد لمادة النفط الثقيلة. الموديل الرياضي يصف توزيع تراكيز المواد المتفاعلة والناجمة, نسبة التحول, وتوزيع درجة الحرارة مع الزمن وطول المفاعل. أثبتت النتائج وجود تطابق كبير بين النتائج العملية والنظرية بنسبة انحراف بين (1,93-14,51)%.

### NOMENCLATURE

| Symbo l        | Definition                           | Units                | Symbo l          | Definition                                               | Units            |
|----------------|--------------------------------------|----------------------|------------------|----------------------------------------------------------|------------------|
| A              | Aromatics                            | (-)                  | K <sub>eq</sub>  | Reaction equil. constant                                 | (-)              |
| A°             | Pre-exponential factor               | (-)                  | LHSV             | Liquid hour space velocity                               | hr <sup>-1</sup> |
| A <sub>i</sub> | Aromatics(6,7,8,9) carbon atom       | (-)                  | Mwt              | Molecular weight                                         | g/gmole          |
| C <sub>N</sub> | Naphthenes concentration             | mole/cm <sup>3</sup> | N <sub>i</sub>   | Naphthene (5,6,7,8,9) C-atom                             | (-)              |
| C <sub>n</sub> | Initial concentration of species n   | mole/cm <sup>3</sup> | n-P <sub>i</sub> | Paraffine(5,6,7,8,9,10)C - atom                          | (-)              |
| C <sub>n</sub> | Concentration of species n           | mole/cm <sup>3</sup> | P                | Paraffin                                                 | (-)              |
| C <sub>p</sub> | Specific heat                        | J/mole.°C            | P <sub>a</sub>   | Total pressure                                           | atm              |
| E <sub>a</sub> | Activation energy                    | kJ/mole              | R                | Gas constant                                             | J/mole.K         |
| F <sub>A</sub> | Molar flow rate of component A       | mole/hr              | r <sub>i</sub>   | Reaction rate of species i                               | mole/gcat . hr   |
| F <sub>n</sub> | Initial molar flow rate of species n | mole/hr              | r <sub>1</sub>   | Reaction rate for paraffin's dehydrocyclization reaction | mole/gcat . hr   |

|                         |                                                 |                  |            |                                                      |                                      |
|-------------------------|-------------------------------------------------|------------------|------------|------------------------------------------------------|--------------------------------------|
| $F_n$                   | Molar flow rate of species n                    | mole/hr          | $r_2$      | React. rate for naphthene's dehydrogenation reaction | mole/gcat . hr                       |
| f                       | Weight flow rate                                | g / hr           | $r_3$      | Reaction rate for paraffin's hydrocracking reaction  | mole/gcat. hr                        |
| G                       | Gases                                           | ( - )            | T          | Reaction temperature                                 | °C                                   |
| GC                      | Gas chromatography                              | ( - )            | T*         | Initial temperature                                  | °C                                   |
| H <sub>2</sub>          | Hydrogen                                        | ( - )            | V          | Volume of gas adsorbed at the equilibrium pressure   | cm <sup>3</sup>                      |
| $\Delta H_r$            | Heat of i th reaction                           | J/ mole          | $V_o$      | Volume of gas adsorbed                               | cm <sup>3</sup>                      |
| H <sub>2</sub> /H.<br>C | Hydrogen to hydrocarbon mole ratio              | ( - )            | $V_C$      | Volume of catalyst                                   | cm <sup>3</sup>                      |
| iso-P                   | Iso-paraffins                                   | ( - )            | W          | Weight of catalyst                                   | kg                                   |
| k                       | Reaction rate constant                          | hr <sup>-1</sup> | WHS        | Weight hour space velocity                           | hr <sup>-1</sup>                     |
| $k_1$                   | Rate constant for paraffin's cyclization        | hr <sup>-1</sup> | $Y_i$      | Molar composition of species i (A, N, and P)         | ( - )                                |
| $k_2$                   | Rate constant for naphthenes dehydrogenation    | hr <sup>-1</sup> | zt         | Length of reactor                                    | cm                                   |
| $k_3$                   | Rate constant for naphthenes hydroisomerization | hr <sup>-1</sup> | $\Delta z$ | Integration step for the reactor length              | ( - )                                |
| $k_4$                   | Rate constant for paraffins hydrocracking       | hr <sup>-1</sup> | C          | Porosity of catalyst bed                             | (-) cm <sup>3</sup> /cm <sup>3</sup> |

## INTRODUCTION

Catalytic reforming of heavy naphtha is a very important process for producing high octane gasoline, aromatic feedstock and hydrogen in petroleum-refining and petrochemical industries. Catalytic naphtha reforming is the process which converts low octane compound in naphtha to high-octane gasoline components, without changing carbon numbers in the molecule. This is achieved mainly by conversion of straight chain naphtha to iso-paraffins and aromatics over a solid catalyst [1, 2].

During catalytic reforming long chain hydrocarbons are rearranged through isomerization, hydrogenation, dehydrocyclization and dehydrogenation reactions. These reactions occur on acid and/or metal sites and they demand the use of bifunctional catalysts. The acid function is typically provided by a solid support such as chlorinated alumina (Al<sub>2</sub>O<sub>3</sub>-Cl) and the metal function by a noble metal. The metal component is active for the hydrogenation and dehydrogenation reactions while the support has the acid strength necessary to promote the isomerization reactions. Synergetic action of both kinds of active sites promotes

other reactions such as dehydrocyclization via a bifunctional reaction mechanism. Undesirable reactions such as hydrocracking and hydrogenolysis also occur lowering the yield of valuable products and deactivating the catalyst by the formation of coke on the active sites [2, 3, 4].

The metals used with Pt/ Al<sub>2</sub>O<sub>3</sub> catalyst other than Re are Sn, Ge, and Ir. These additives modify the activity, selectivity and stability of the catalyst. These metals are used as bimetallic catalyst. The effects of the additives on the reforming reaction are [5, 6, 7, and 8]:

- (I) They decrease the deep dehydrogenation capacity of (Pt) and thus decrease the formation of unsaturated coke precursors.
- (II) They decrease the hydrogenolysis capacity and therefore also decrease the formation of light gases.
- (III) They modify the concentration of surface hydrogen. This has an effect on relative production of different reaction intermediates and therefore on the final reaction selectivity.
- (IV) A portion of the additives remains oxidized on the surface and modifies the amount and strength of the acid site of the support.

This type of bimetallic naphtha reforming catalyst makes a big leap forward in the technology of reforming catalyst and it improves its properties, Pt-Ir/ Al<sub>2</sub>O<sub>3</sub>-Cl, Pt-Sn/ Al<sub>2</sub>O<sub>3</sub>-Cl, and Pt-Ge/ Al<sub>2</sub>O<sub>3</sub>-Cl being the most remarkable followers [4, 5, and 9].

Recently there has been a renewed interest in the reforming process, first, because reformat is a major source of aromatics in gasoline, and second, because of the new legislation concerning benzene and aromatics content in commercial gasoline. In this sense, reformers have reduced the severity of the industrial reforming plants in order to decrease the amount of aromatics in gasoline; however it adversely affects the octane. Therefore, to design new plants and optimize the existing ones, an appropriate mathematical model for simulating the industrial catalytic reforming process is needed [6, 7, 10, 11, 12]. The aims of this work is to produce high octane aromatics from Iraqi heavy naphtha by using prepared bi-metallic catalysts in a fixed bed reactor under various ranges of temperature and weight hour space velocity. On the other hand, predict and develop a mathematical model to describe the catalytic reforming reactions, reaction rate and optimum operating conditions for the reforming catalysts.

## **EXPERIMENTAL WORK**

### **Materials**

Iraqi heavy naphtha with 0.733 specific gravity was supplied by Al-Dura refinery. The properties of this naphtha as shown in Table (1). Nitrogen purchased from Dijlah factory, was analyzed by G.C and confirms its purity of 99%. G.C analysis for purchased from Al-Mansor plant, shows that its purity of 99.9%. To reduce oxygen and water impurities an molecular sieve type (5A) has been installed on the hydrogen line.

Table (1) the properties of heavy naphtha (Al-Dura refinery).

| Property                     | Unit   | Data  |
|------------------------------|--------|-------|
| Specific Gravity at 15.6 °C  | -      | 0.733 |
| API                          | -      | 61.7  |
| <b>Distillation</b>          |        |       |
| I.B.P                        | °C     | 60    |
| 10 vol % distilled           | °C     | 88    |
| 20 vol% distilled            | °C     | 94    |
| 30 vol% distilled            | °C     | 106   |
| 40 vol% distilled            | °C     | 110   |
| 50 vol % distilled           | °C     | 117   |
| 60 vol% distilled            | °C     | 124   |
| 70 vol% distilled            | °C     | 132   |
| 80 vol% distilled            | °C     | 140   |
| 90 vol % distilled           | °C     | 147   |
| F.B.P                        | °C     | 178   |
| Total distillate             | vol%   | 98.5  |
| Total recovery               | vol%   | 99.5  |
| Residue                      | vol%   | 1     |
| Loss                         | vol%   | 0.5   |
| Sulfur Content               | ppm    | 3     |
| Mwt.                         | g/gmol | 108   |
| Total Paraffin               | vol %  | 60    |
| Total naphthene and aromatic | vol %  | 40    |

#### CATALYSTS

Pt/  $\gamma$ -Al<sub>2</sub>O<sub>3</sub> (RG 412), Pt-Re/  $\gamma$ -Al<sub>2</sub>O<sub>3</sub> (RG 482) catalysts are supplied from Al-Dura refinery. The two bi-metals catalysts were prepared in our laboratory. The physical and chemical properties of all catalysts were measured and the results are shown in Table (2).

#### Preparation of Platinum-Iridium / Alumina Catalyst

The Pt-Ir/Al<sub>2</sub>O<sub>3</sub> catalyst was prepared by impregnation the parent catalyst (Pt/Al<sub>2</sub>O<sub>3</sub>) with Iridium chloride (IrCl<sub>3</sub>) in order to reach final concentration of 0.5 wt% of Pt and 0.1 wt% of Ir [8].

Iridium chloride was added to the slurry solution of HCl and support and gently stirred for 1 hr at room temperature. The slurry was left into water bath at 70 °C. Then dried at 120 °C overnight. The catalysts were finally calcined in air at 300 °C for 4 hrs and then reduced by flowing hydrogen at (60 cm<sup>3</sup>/min) at 500 °C for 4 hrs. Heating ramps were programmed every 10 °C /min.

#### Preparation of Platinum-Tin / Alumina Catalyst

The Pt-Sn/ Al<sub>2</sub>O<sub>3</sub> catalyst was prepared by impregnation of the parent catalyst (Pt/Al<sub>2</sub>O<sub>3</sub>) with tin chloride (SnCl<sub>2</sub>.2H<sub>2</sub>O) in order to reach final concentration of 0.35 wt% Pt and 0.3 wt% of Sn [9].

Tin chloride was dissolved in heated deionized water and heated for 30 min at 70 °C. An amount of 0.2M of HCl solution was added to the support prior the impregnation step in order to make sure homogeneous distribution of them. Then added to the catalyst and left for 1 hr unstirred, then gently heated at 70 °C in order to evaporate excess liquid. The catalyst was finally dried at 120°C for 12 hrs and calcined in air at 500 °C for 4 hrs. Then, the catalyst was reduced in flowing H<sub>2</sub> stream of 60 cm<sup>3</sup>/min for 4 hrs at 500°C.

**Table (2) Physical and chemical properties of commercial and prepared catalysts**

|                                   | Commercial Pt/ $\gamma$ -Al <sub>2</sub> O <sub>3</sub> | Commercial Pt-Re/ $\gamma$ -Al <sub>2</sub> O <sub>3</sub> | Prepared Pt-Sn/ $\gamma$ -Al <sub>2</sub> O <sub>3</sub> | Prepared Pt-Ir/ $\gamma$ -Al <sub>2</sub> O <sub>3</sub> |
|-----------------------------------|---------------------------------------------------------|------------------------------------------------------------|----------------------------------------------------------|----------------------------------------------------------|
| Pt , wt %                         | 0.35                                                    | 0.3                                                        | 0.35                                                     | 0.5                                                      |
| Re, wt %                          | -                                                       | 0.3                                                        | -                                                        | -                                                        |
| Sn ,wt %                          | -                                                       | -                                                          | 0.3                                                      | -                                                        |
| Ir , wt %                         | -                                                       | -                                                          | -                                                        | 0.1                                                      |
| Form                              | Extrudate                                               | Extrudate                                                  | Extrudate                                                | Extrudate                                                |
| Surface Area (m <sup>2</sup> /g)  | 220                                                     | 220                                                        | 205.4                                                    | 219.9                                                    |
| Pore Volume (cm <sup>3</sup> /g)  | 0.57                                                    | 0.6                                                        | 0.68                                                     | 0.61                                                     |
| Bulk Density (g/cm <sup>3</sup> ) | 0.66                                                    | 0.69                                                       | 0.624                                                    | 0.67                                                     |

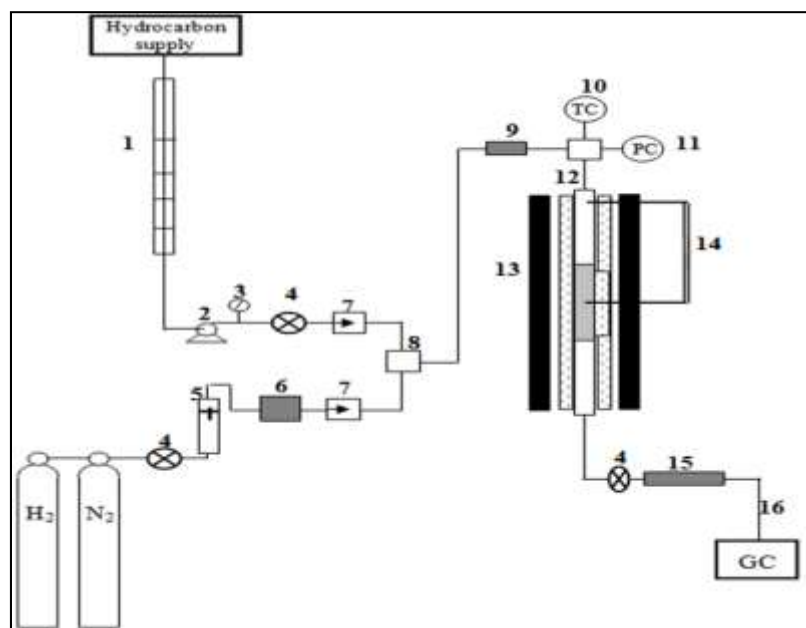
### Heavy Naphtha Catalytic Reforming Unit

The catalytic activities studies were carried out in a conventional continuous flow vertical tubular reactor, the dimensions were 20mm internal diameter, 30mm external diameter and 68cm height (reactor volume 214 cm<sup>3</sup>). The reactor was charged for each experiment with 50g (catalyst bed 22 cm) of catalyst located in the middle zone, while, the upper and lower zones were filled with glass beads. Figure (1) shows the pilot plant of catalytic reforming unit.

### Operating Procedure

All the catalysts were originally in the form of extrudate. Each type was activated inside the reactor, just prior running the tests runs. The reactivation it was 450 and 500 °C for 4 hr respectively in a current of hydrogen at 1 atm pressure and flow ratio of 60 and 80 cm<sup>3</sup>/min. Heavy naphtha pumped under pressure to the reforming unit. Hydrogen mixed with hydrocarbon prior entering the reactor inlet. The mixture was preheated, and then admitted through the catalyst bed. The products were cooled and collected in a separator in order to exhaust the gases to the atmosphere and collect the condensed liquid from bottom of the separator. Products samples were analyzed using gas chromatograph type Shimadzu 2014 GC.

The reforming process was tested at different temperatures (480, 490, 500, and 510 °C), and 6 atm. The weight hourly space velocities were varied at (1, 1.5, and 2 hr<sup>-1</sup>), and 4:1 hydrogen to hydrocarbon molar ratio. For each run a fresh catalyst was used; therefore, the effect of catalyst deactivation was neglected.



|                               |                                    |
|-------------------------------|------------------------------------|
| 1-Metering burette            | 9- Feed preheating zone            |
| 2-Dosing pump                 | 10 - Temperature controller system |
| 3-Liquid flow meter           | 11- Pressure controller system     |
| 4-Needle valve                | 12- Stainless steel reactor        |
| 5- H <sub>2</sub> flow meter  | 13- Heating furnace                |
| 6- 5A – Molecular sieve dryer | 14- Thermocouples system           |
| 7- One way valve              | 15- Cooling system                 |
| 8- Mixing section             | 16- Gas chromatography             |

Figure (1) Schematic diagram of the experimental apparatus of catalytic reforming pilot plant.

### SIMULATION AND MATHEMATICAL MODEL

Mathematical modeling in the reforming process has increasingly shown an important tool in petroleum refining industries. It because crucial in developing proper design of new reactor and revamp of existing ones. Modeling can be used to

optimize operating conditions, analyze the effects of process variables, and enhance unit performance. In the present work mathematical models of catalytic reforming reactor can be of complexity which generally depends on description of reactants flow along the reactor, kinetic model of a chemical reaction and mass and energy balance (describe reformate composition).

### Model Description and Assumptions

The main aim of the present study is to analyze the kinetics of reforming process by assessing the effect of reaction time and reaction temperature on the substrate content in the course of process which involves heavy naphtha as raw material. Therefore, three groups of compounds are found which are: paraffins (normal and iso), naphthenes (N), and aromatics (A). Then, the physical model for catalytic reforming with mass and energy balances for the element combining kinetic thermodynamic, concentration, and temperature distributions along the reactor length can be calculated.

In developing the catalytic reforming reactor model the the following assumptions are taken into account:

- ❖ Steady state operation and plug flow isothermal operation.
- ❖ The pressure is constant throughout the reactor.
- ❖ The surface reaction was the limiting step.
- ❖ Density of reactant and products are constant.
- ❖ The temperature and concentration gradients along the radial direction can be neglected and only axial direction are considered.
- ❖ All the reforming reactions rates are first order (proved experimentally), all the rate equations are linear pseudo-monomolecular in nature and constant catalyst activity for calculation.

### Reaction Kinetics

According to the present work investigation, analysis and monitoring of the heterogeneous reaction (consecutive and parallel) of heavy naphtha catalytic reforming, the suggested reactions network are represented schematically in Figure (2).

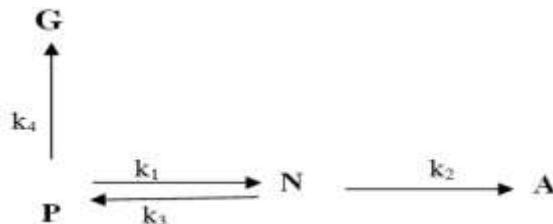
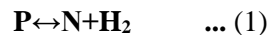
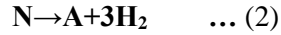


Figure (2) the suggested reactions network of heavy naphtha reforming of the present work.





The reaction rate is considered to follow simple power law kinetic expression for above reactions [10]:

$$r_1 = k_1 C_P - k_3 C_N P_{H_2} \dots (4)$$

$$r_2 = k_2 C_N \quad \dots (5)$$

$$r_3 = k_4 C_P \quad \dots (6)$$

In general form  $r_i = k_i C_i^n \quad \dots (7)$

where,  $k_i = A_i \text{EXP} \left( \frac{-E_a}{RT} \right) \dots (8)$

The reaction rate constant  $k_i$  confirms the Arrhenius expression [10]:

$$\text{Ln} k_i = \text{Ln} A_i - \frac{E_a}{RT} \quad \dots (9)$$

The reaction equilibrium constants  $K_{eq} = k_1/k_3$ . Therefore, equilibrium constant can be calculated by the following thermodynamic relation [11]:

$$K_{eq} = \text{EXP} \left( \frac{-\Delta G}{RT} \right) \quad \dots (10)$$

The kinetic expression is to be linear (first order with respect to reactants) under the present reactions.

## KINETIC REACTION MODEL

### Mass Balance

To develop a reaction model for an integral reactor, a material balance is made over the cross section of a very short segment of the tubular catalyst bed, as shown in Figure (3):

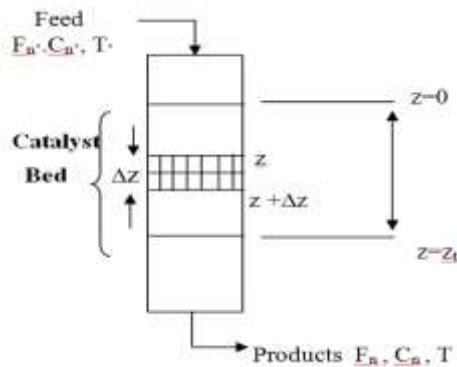


Figure (3) Segment of tubular reactor of reaction model.

Then, the resulting equation [12] is:

$$F_N - F_N - V_{PP} (1-C) (-r_i) = 0 \quad \dots (11)$$

As  $\Delta z \rightarrow 0$ , the differential material balance reduces to:

$$\frac{dF_n}{dw} = -r_i \quad \dots (12)$$

Where:  $dw = dv \rho (1-C)$

Now, the reaction rate equations can now be developed for each component in heavy naphtha feed stocks (Paraffins, Naphtenes and Aromatics) as follows:-

$$\frac{dF_P}{dw} = k_3 C_N - (k_4 + k_1) C_P \quad \dots (13)$$

$$\frac{dF_N}{dw} = k_1 C_P - (k_3 + k_2) C_N \quad \dots (14)$$

$$\frac{dF_A}{dw} = k_2 C_N \quad \dots (15)$$

A final modification to the left-hand side of equations (13) to (15) is made by defining a space time variable,  $\theta$ , as:

$$\theta = w/f \quad \dots (16)$$

For a constant feed rate, an incremental section of catalyst bed, may expressed as:

$$dw=f.d\theta \quad \dots (17)$$

Substituting equation (17) in above equations (13, 14, and 15) gives:

$$\frac{dF_P}{d\theta} = k_3 F_N - (k_4 + k_1) F_P \quad \dots (18)$$

$$\frac{dF_N}{d\theta} = k_1 F_P - (k_3 + k_2) F_N \quad \dots (19)$$

$$\frac{dF_A}{d\theta} = k_2 F_N \quad \dots (20)$$

### Energy Balance

The equation used to estimate the temperature profile along the reactor is obtained from an energy balance over the differential reactor control volume [13].

$$f.p.C_p dT = r_{P \leftrightarrow N} \Delta H_{r, P \leftrightarrow N} dV + r_{N \leftrightarrow A} \Delta H_{r, N \leftrightarrow A} dV + r_{P \rightarrow G} \Delta H_{r, P \rightarrow G} dV \dots (21)$$

Substituting equations (17) in to above equation yield:-

$$\frac{dT}{d\theta} = \frac{1}{\rho C_P} \left( \begin{array}{l} r_{P \leftrightarrow N} \Delta H_{r, P \leftrightarrow N} \\ + r_{N \rightarrow A} \Delta H_{r, N \rightarrow A} \\ + r_{P \rightarrow G} \Delta H_{r, P \rightarrow G} \end{array} \right) \quad \dots (22)$$

The above differential equation is taken to be as first order and this is improved experimentally as:-

$$-r_i = k_i C_i^n \quad \dots (7)$$

Taking Ln for both side of above equation yield:

$$\text{Ln}(-r_i) = \text{Ln}k_i + n\text{Ln}C_i \quad \dots (23)$$

By plotting Ln (-r<sub>i</sub>) vs. LnC<sub>i</sub>, then, the behaviors of first order must be straight line (tan 45° = 1) as shown in Figures (4 and 5) for different reaction and different catalyst. These two figures are just samples for some selected types of both catalysts.

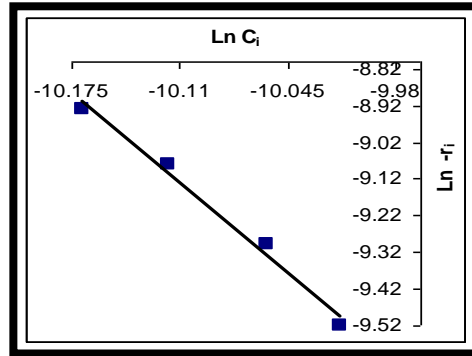
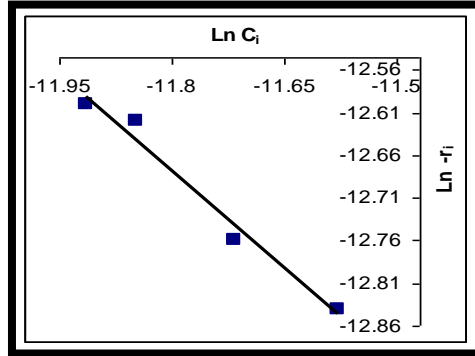


Figure (4) Plot for N+H<sub>2</sub>→P for Pt-Ir catalyst at 1.5 hr<sup>-1</sup>

Figure (5) Plot for P→N+H<sub>2</sub> for Pt-Sn catalyst at 1.5 hr<sup>-1</sup>

### PROCESS MODEL

The physical model for catalytic reforming axial flow reactor is shown in Figure (3). The following ordinary differential equations for mass and energy balance were integrated through each reactor bed to describe reformate composition and temperature profile along the length of the reactor. The system is numerically solved by method of finite difference approach with explicit solution of all the differential equation in the mathematical model. The schematic step of reactor models has shown in Figure (6).

**For Mass balance [14]:**

$$\frac{dY_i}{dZ} = \sum_{i=1}^m \frac{MW}{z.WHSV} (-r_i) \quad \dots (24)$$

If substitute's heavy naphtha components (paraffin, naphthene, and aromatic) then, equation (24) become:

$$\frac{dY_P}{dZ} = \frac{MW}{z.WHSV} [r_{N \rightarrow P} - (r_{P \rightarrow N} + r_{P \rightarrow G})] \quad \dots (25)$$

$$\frac{dY_N}{dZ} = \frac{MW}{z.WHSV} [r_{P \rightarrow N} - (r_{N \rightarrow P} + r_{N \rightarrow A})] \quad \dots (26)$$

$$\frac{dY_A}{dZ} = \frac{MW}{z.WHSV} (r_{N \rightarrow A}) \quad \dots (27)$$

**For energy balance:**

$$\frac{dT}{dZ} = S \frac{\sum_{i=1}^m r_i (-\Delta H_{r_i})}{\sum_{i=1}^m f_i C_{P_i}} \quad \dots (28)$$

$$\frac{dT}{dZ} = \frac{S}{\sum_{i=1}^m f_i C_{P_i}} \left[ \begin{array}{l} r_{P \rightarrow N} (-\Delta H_{r, P \rightarrow N}) \\ + r_{N \rightarrow A} (-\Delta H_{r, N \rightarrow A}) \\ + r_{N \rightarrow P} (-\Delta H_{r, N \rightarrow P}) \\ + r_{P \rightarrow G} (-\Delta H_{P \rightarrow G}) \end{array} \right] \quad \dots (29)$$

$$\Delta H^{\circ}_{r,T} = \Delta H^{\circ}_{r,298} + \int_{298}^T \Delta C_p dT \quad \dots (30)$$

The results of heat reactions estimations are represented in Table (3).

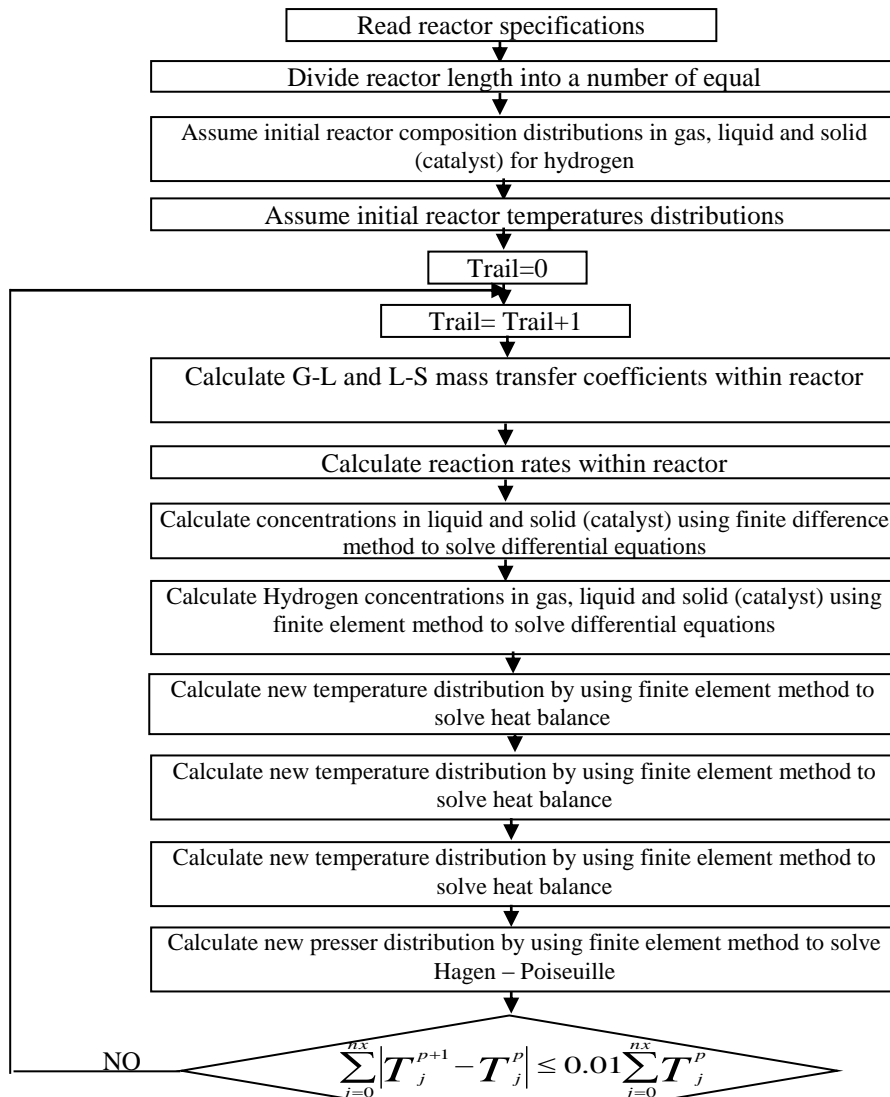


Figure (6) a schematic step of reactor models.

Table (3) Results of analysis of heat of reaction.

| $\Delta H^{\circ}_r$ (J/mole H <sub>2</sub> ) |          |         |          |          |
|-----------------------------------------------|----------|---------|----------|----------|
| Reaction                                      | 480 °C   | 490 °C  | 500 °C   | 510 °C   |
| N + H <sub>2</sub> → P                        | -54393.3 | 54238.5 | -53903.7 | -53648.5 |
| N → A + 3H <sub>2</sub>                       | 73119.9  | 73207.8 | 73291.5  | 73361.2  |

| Reaction                                                     | Ea/R   | Ea (kcal/mol) | A°                    |
|--------------------------------------------------------------|--------|---------------|-----------------------|
| <b>Pt-Sn/<math>\gamma</math>-Al<sub>2</sub>O<sub>3</sub></b> |        |               |                       |
| P → N + H <sub>2</sub>                                       | 15084  | 125.40        | 7.927*10 <sup>8</sup> |
| N + H <sub>2</sub> → P                                       | 10674  | 88.74         | 6.733*10 <sup>5</sup> |
| N → A + 3H <sub>2</sub>                                      | 9822.2 | 81.63         | 7.997*10 <sup>5</sup> |
| P + H <sub>2</sub> → 2G                                      | 11905  | 98.95         | 5.803*10 <sup>6</sup> |
| <b>Pt-Ir/<math>\gamma</math>-Al<sub>2</sub>O<sub>3</sub></b> |        |               |                       |
| P → N + H <sub>2</sub>                                       | 15802  | 131.39        | 1.173*10 <sup>9</sup> |

|                          |        |        |                    |
|--------------------------|--------|--------|--------------------|
| $N + H_2 \rightarrow P$  | 11400  | 94.77  | $1.005 \cdot 10^6$ |
| $N \rightarrow A + 3H_2$ | 9841.3 | 81.80  | $1.561 \cdot 10^6$ |
| $P + H_2 \rightarrow 2G$ | 13859  | 115.19 | $3.616 \cdot 10^6$ |

#### Estimation of Reaction Kinetic Parameters

The apparent activation energy ( $E_a$ ) is established from Arrhenius equation that satisfies the relationships between rate constant and reaction temperature as given in equations (7, 8, and 9). From plot of  $\ln(k)$  vs.  $(1/T)$  as shown in Figures (7 and 8). The values of activation energy were calculated from the slope represented by  $(-E_a/R)$  and the intercept represented by  $\ln(A_0)$  let us to determine the value of pre-exponential factor. Results of each catalysts type are listed in Table (4).

**Table (4) Activation energy values and pre-exponential Factor for bi-metal catalysts.**

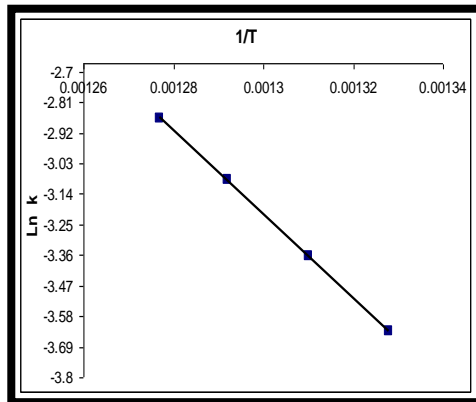


**Figure (7)** Arrhenius plot for the reaction  $P \rightarrow N + H_2$  for Pt-Sn/ $\gamma$ -Al<sub>2</sub>O<sub>3</sub>.

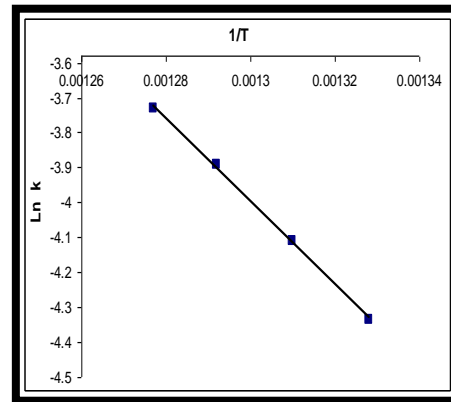


**Figure (8)** Arrhenius plot for the reaction  $P + H_2 \rightarrow 2G$  for Pt-Sn/ $\gamma$ -Al<sub>2</sub>O<sub>3</sub>.

## RESULTS AND DISCUSSION

### Effect of Temperature

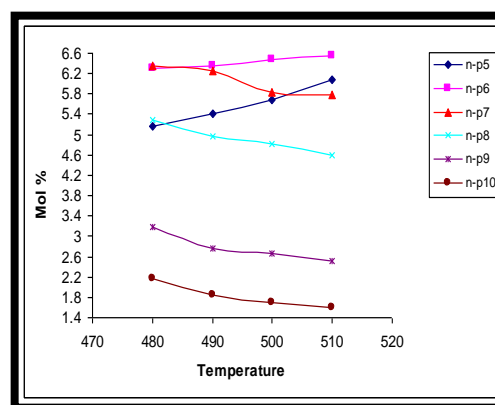
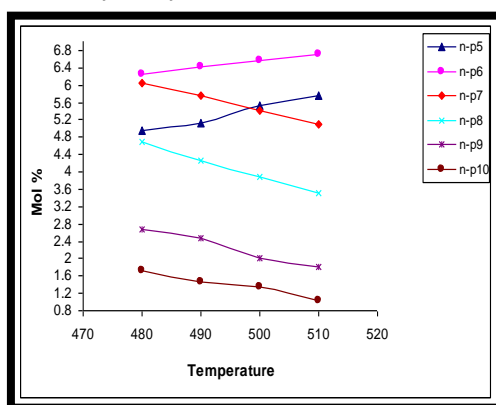
Figures (9 and 10) show that the concentration of light components (n-P<sub>5</sub> and n-P<sub>6</sub>) are increased with an increase in the reaction temperature and the heavier components concentration % decrease as reaction temperatures increases. This result is attributed to the dehydrocyclization reaction which is favored at higher reaction temperature and higher molecular weight of carbon number [16].

Figures (11 and 12) show that the iso-P<sub>6</sub> increases with temperature increase, but, iso-P<sub>7</sub> content increases as reaction temperature increases and then decreases at higher temperature. Also, the heavier paraffin's contents decreases with temperature increase.

Figures (13 and 14) shows that naphthenes mole % decreases as reaction temperature increases, since the conversion of naphthenes to aromatics is the primary naphthene reaction and is regarded the most favorable amongst with all other reactions in catalytic reforming. It is important to mention here that the reactivity of dehydrogenation reactions increases with an increase in naphthenes carbon number [17].

Figures (15 and 16), show that the mole percentage of aromatics components increases as the reaction temperatures increased. This behavior can be explained on the basis of that the dehydrogenation of naphthenes and dehydrocyclization of paraffin's became faster with increasing of temperature and carbon number.

The comparison between the performance of the two types of catalysts (Pt-Sn/ $\gamma$ -Al<sub>2</sub>O<sub>3</sub>, Pt-Ir/ $\gamma$ -Al<sub>2</sub>O<sub>3</sub>) shows that the first type is better than the second one because the addition of tin has enhance the selectivity of isomerization, and increases the aromatization reaction in accord with the work of Bednarova et al. [18]. Therefore, in the present investigation, it is clear that the aromatic mole% produced from the reaction is about 30.4 mole % at 510 °C and 26.56 mole% for the second type of catalyst under the same condition. Then, it can be concluded that the use of tin with platinum will lead to improvement of the dehydrogenation and dehydrocyclization reactions rather than iridium.



Reforming Reactions of Iraqi Heavy  
Naphtha Using Pt-Sn/ $\gamma$ -Al<sub>2</sub>O<sub>3</sub> and Pt-  
Ir/ $\gamma$ -Al<sub>2</sub>O<sub>3</sub> Catalysts

**Figure (9)** Effect of temperature on the mole % of n-Paraffins components at WHSV of (1 hr<sup>-1</sup>) catalytic.

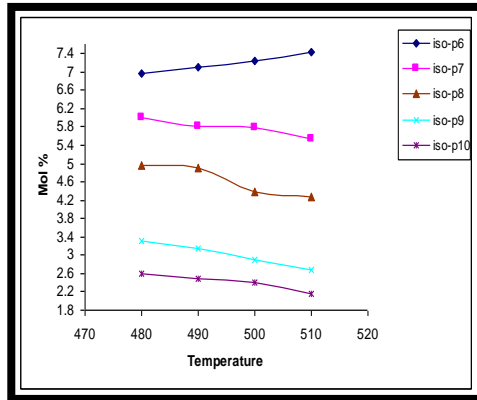


**Figure (10)** Effect of temperature on mole % of n-Paraffins components at for (Pt-Sn /  $\gamma$ -Al<sub>2</sub>O<sub>3</sub>) WHSV of (1 hr<sup>-1</sup>) for (Pt-Ir /  $\gamma$ -Al<sub>2</sub>O<sub>3</sub>) catalyst.

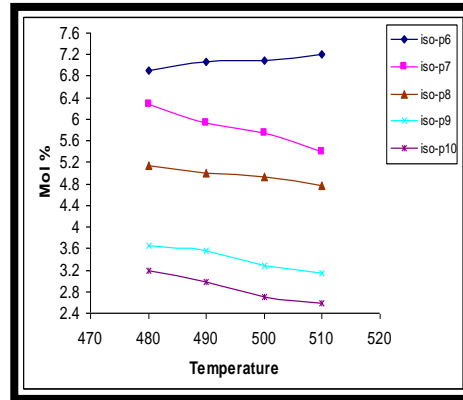


**Figure (11)** Effect of temperature on the mole % of iso-Paraffins components at WHSV of (1 hr<sup>-1</sup>) for (Pt-Sn /  $\gamma$ -Al<sub>2</sub>O<sub>3</sub>) catalyst.

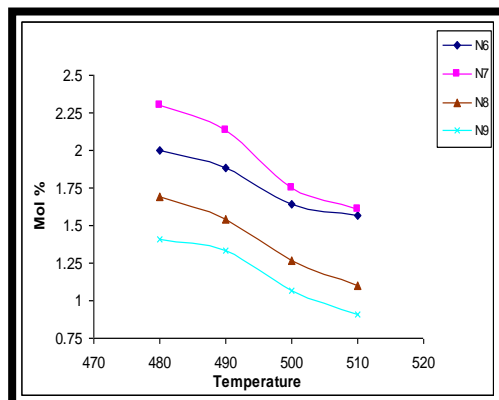


**Figure (13)** Effect of temperature on the mole % of naphthenes components at WHSV of (1 hr<sup>-1</sup>) for (Pt-Sn /  $\gamma$ -Al<sub>2</sub>O<sub>3</sub>) catalyst.

**Figure (12)** Effect of temperature on the mole % of iso-Paraffins components at WHSV of (1 hr<sup>-1</sup>) for (Pt-Ir /  $\gamma$ -Al<sub>2</sub>O<sub>3</sub>) catalyst.

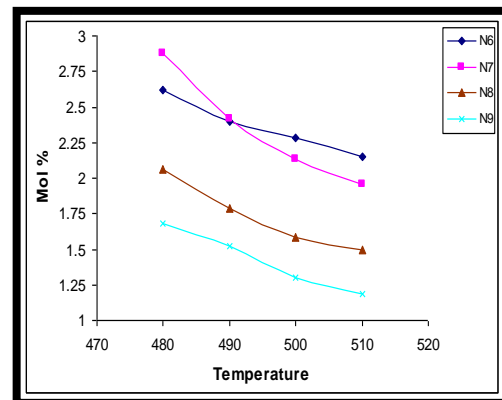


**Figure (14)** Effect of temperature on the mole % of naphthenes components at WHSV of (1 hr<sup>-1</sup>) for (Pt-Ir /  $\gamma$ -Al<sub>2</sub>O<sub>3</sub>) catalyst.

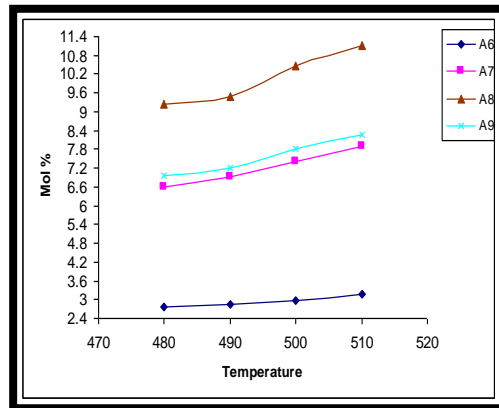


**Figure (15)** Effect of temperature on the mole % of aromatics components at WHSV of (1 hr<sup>-1</sup>) for (Pt-Sn /  $\gamma$ -Al<sub>2</sub>O<sub>3</sub>) catalyst.

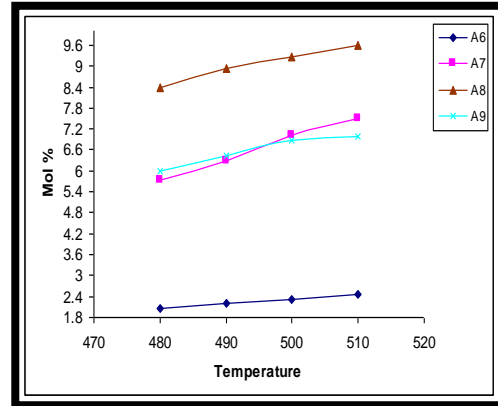


**Figure (16)** Effect of temperature on the mole % of aromatics components at WHSV of (1 hr<sup>-1</sup>) for (Pt-Ir /  $\gamma$ -Al<sub>2</sub>O<sub>3</sub>) catalyst.

### Effect of Weight Hour Space Velocity (WHSV)

The influence of WHSV was studied at (1, 1.5, and 2 hr<sup>-1</sup>), and temperature of (510 °C), which gave the highest aromatics yield. Figures (17 and 18) have clearly illustrated that the mole% of light component (n-P<sub>5</sub> and n-P<sub>6</sub>) decreases as WHSV increases; this behavior is due to the slow rate of hydrocracking reaction. Therefore, the increase in WHSV causes a decrease in the residence time, which offers plenty of contact time of feedstock with the catalyst inside reactor, which latter lead to an effective conversion of n-paraffins [19]. It can also observe that the heavier paraffins reactivity decreases as WHSV increases.

Figures (19) and (20) show that the iso-paraffins components decrease with increasing of WHSV, but this decrease is less than the decreases in n-paraffin. Such conclusion is attributed to the fact that selectivity of paraffin's isomerization reactions at typical reforming operating condition is relatively insignificant to space velocity. The same conclusion was noted by Jenkins et al. [20].

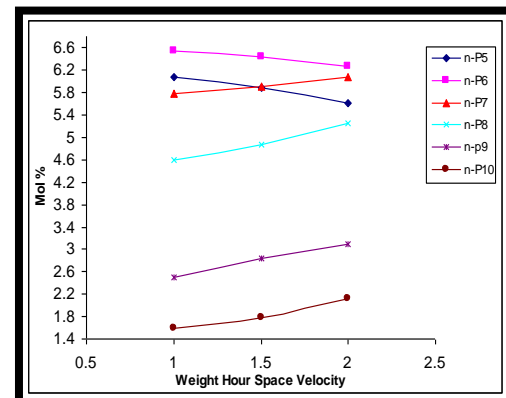
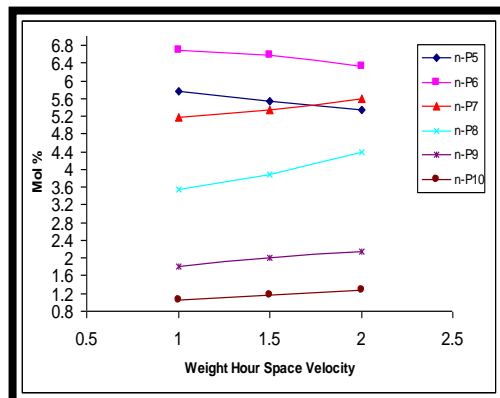


**Figure (17)** Effect of weight hour space velocity on the mole % of n-Paraffins components at 510 °C for (Pt-Sn /  $\gamma$ -Al<sub>2</sub>O<sub>3</sub>) catalyst.

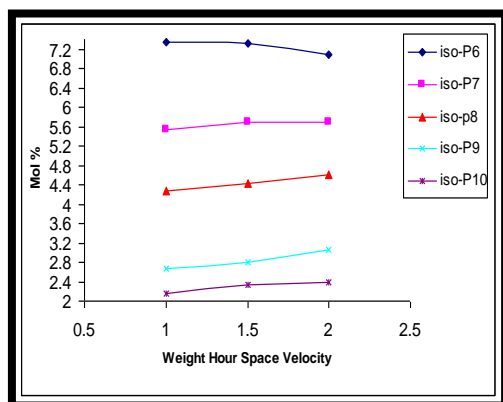


**Figure (18)** Effect of weight hour space velocity on the mole % of n-Paraffins components at 510 °C for (Pt-Ir /  $\gamma$ -Al<sub>2</sub>O<sub>3</sub>) catalyst.

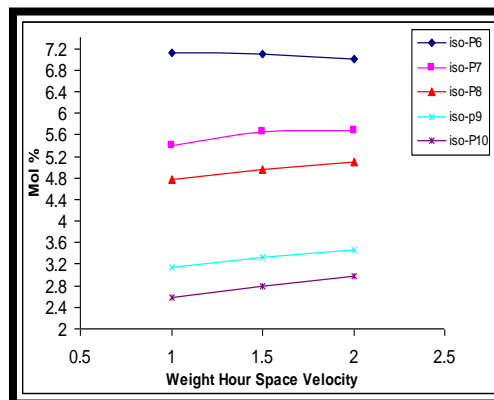


**Figure (19)** Effect of weight hour space velocity on the mole % of iso-Paraffins components at 510 °C for (Pt-Ir /  $\gamma$ -Al<sub>2</sub>O<sub>3</sub>) catalyst.

**Figure (20)** Effect of weight hour space velocity on the mole % of iso-Paraffins components at 510 °C for (Pt-Sn /  $\gamma$ -Al<sub>2</sub>O<sub>3</sub>) catalyst.

Figures (21 and 22) show same general trend of decreasing of naphthenes components conversion to aromatics via dehydrogenation reaction (mole % increase, means reactivity decrease) with increasing WHSV. The slight decrease in this trend is directly to the dehydrogenation reaction which is the fastest reaction among all heavy naphtha reforming reactions [3, 13].

From the results of Figures (23 and 24) it is observed that, increasing of WHSV will lead to a decrease in the aromatics yield. It is important to mention here that the aromatics components are produced from dehydrogenation of naphthenes which is not affected too much with WHSV and from dehydrocyclization reaction of Paraffins (n and iso), where, it is the slowest reaction and is affected by the increasing of WHSV and that attributed to the low contact time with the catalyst [21].

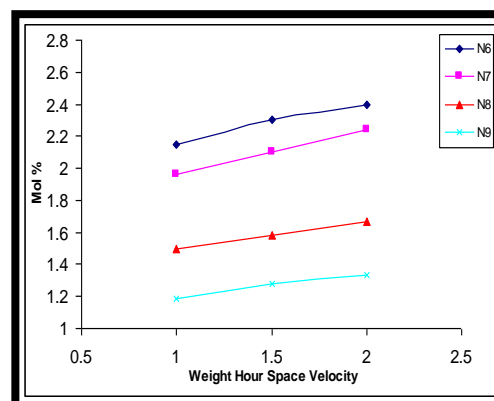
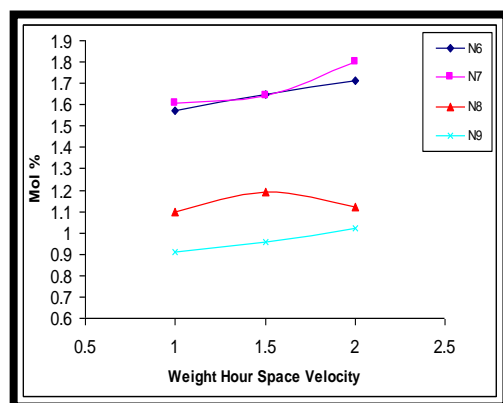


**Figure (21)** Effect of weight hour space velocity on the mole % of naphthenes components at 510 °C for (Pt-Ir /  $\gamma$ -Al<sub>2</sub>O<sub>3</sub>) catalyst.

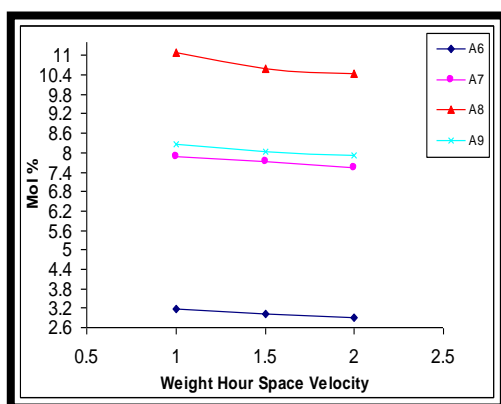


**Figure (22)** Effect of weight hour space velocity on the mole % of naphthenes components at 510 °C for (Pt-Sn /  $\gamma$ -Al<sub>2</sub>O<sub>3</sub>) catalyst.

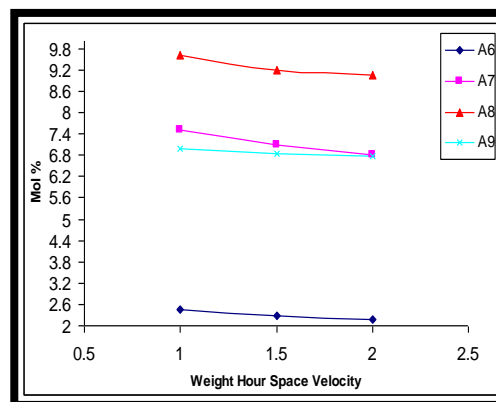


**Figure (23)** Effect of weight hour space velocity on the mole % of aromatics components at 510 °C for (Pt-Sn /  $\gamma$ -Al<sub>2</sub>O<sub>3</sub>) catalyst.

**Figure (24)** Effect of weight hour space velocity on the mole % of aromatics components at 510 °C for (Pt-Ir /  $\gamma$ -Al<sub>2</sub>O<sub>3</sub>) catalyst.

### Simulation Results of Mathematical Model

Figures (25 and 26) show the concentration profiles for reactants (Paraffins and Naphthenes) and products (aromatics and gases) for all catalysts types used in the present work at 480 °C and WHSV of 1hr<sup>-1</sup> as an example.

Figures (27 and 28) show the comparison between the experimental and predicted conversion of Paraffins and Naphthenes and Aromatics for all catalysts types. Table (5) represent the comparison between theoretical and experimental data. It was concluded that, the derived model and simulation agrees with the experimental work results according to the suggested scheme of reactions network for heavy naphtha reforming. The comparison between the model and experimental results shows a deviation range of 1.93% to 14.51%.

**Table (5) comparison between theoretical and experimental conversions for bi-metal catalyst at constant WHSV (1hr<sup>-1</sup>) for different reaction temperatures**

| Condition | Components | Pt-Sn / $\gamma$ -Al <sub>2</sub> O <sub>3</sub> |              | Relative deviation % | Pt-Ir / $\gamma$ -Al <sub>2</sub> O <sub>3</sub> |              | Relative deviation % |
|-----------|------------|--------------------------------------------------|--------------|----------------------|--------------------------------------------------|--------------|----------------------|
|           |            | Exp. Conv %                                      | Theo. Conv % |                      | Exp. Conv %                                      | Theo. Conv % |                      |
|           |            |                                                  |              |                      |                                                  |              |                      |

|        |            |       |       |       |       |       |       |
|--------|------------|-------|-------|-------|-------|-------|-------|
| 480 °C | Paraffins  | 6.03  | 6.72  | 10.26 | 3.71  | 4.34  | 14.51 |
| 490 °C | Paraffins  | 7.90  | 8.40  | 6     | 5.52  | 5.54  | 0.36  |
| 500 °C | Paraffins  | 9.66  | 10.40 | 7.11  | 7.18  | 7.02  | 2.28  |
| 510 °C | Paraffins  | 11.84 | 12.78 | 7.35  | 8.65  | 8.82  | 1.93  |
| 480 °C | Naphthenes | 50.16 | 52.51 | 4.47  | 44.40 | 47.29 | 6.11  |
| 490 °C | Naphthenes | 51.10 | 56.84 | 10.10 | 48.17 | 51.85 | 7.10  |
| 500 °C | Naphthenes | 54.75 | 60.84 | 10    | 50.81 | 56.21 | 9.6   |
| 510 °C | Naphthenes | 55.12 | 64.40 | 14.41 | 51.94 | 60.29 | 13.85 |
| 480 °C | Aromatics  | 1.734 | 1.814 | 4.41  | 1.504 | 1.691 | 11.1  |
| 490 °C | Aromatics  | 1.797 | 1.911 | 5.96  | 1.622 | 1.778 | 8.77  |
| 500 °C | Aromatics  | 1.945 | 2.013 | 3.38  | 1.729 | 1.869 | 7.50  |
| 510 °C | Aromatics  | 2.065 | 2.121 | 2.64  | 1.804 | 1.964 | 8.17  |

The predicted temperature profiles using Pt-Sn / $\gamma$ -Al<sub>2</sub>O<sub>3</sub> along bed length at temperatures 480 °C, and 490 °C can be seen in Figures (29 and 30). The results of these Figures give the trend of temperature profile which decreases along the catalyst bed length (distance), for all temperature ranges. This trend agrees with the published results for heavy naphtha catalytic reforming process. Many researches indicate that the temperature decreases along the catalyst bed, because reforming process reactions are, overall, endothermic. For this reason, commercial catalytic reformers are designed with multiple reactors and with heaters between the reactors to maintain reaction temperature at operatable levels [14, 16, 21].

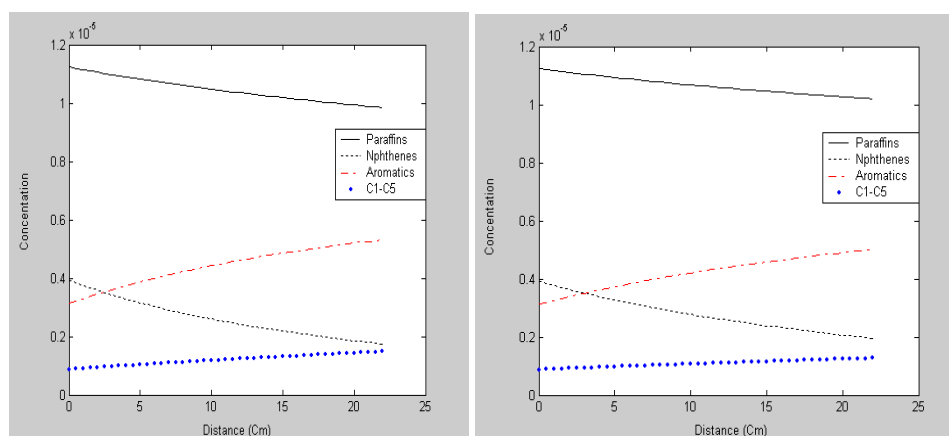


Figure (25) Concentration profiles for (Paraffins, Figure (26) Concentration profiles for (Paraffins,

Naphthenes, Aromatics, and gases) at 480 °C  
and (1 hr<sup>-1</sup>) for (Pt-Sn / γ-Al<sub>2</sub>O<sub>3</sub>) catalyst.

Naphthenes, Aromatics, and gases) at 480 °C  
and (1 hr<sup>-1</sup>) for (Pt-Ir / γ-Al<sub>2</sub>O<sub>3</sub>) catalyst.

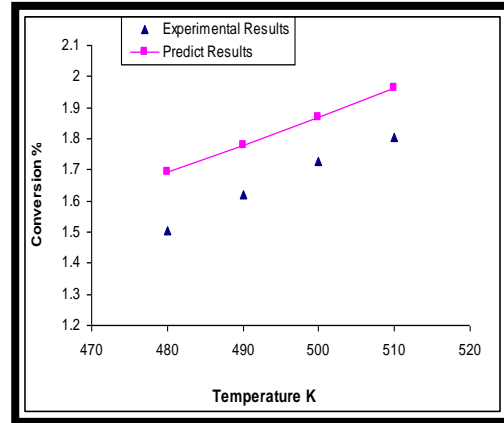
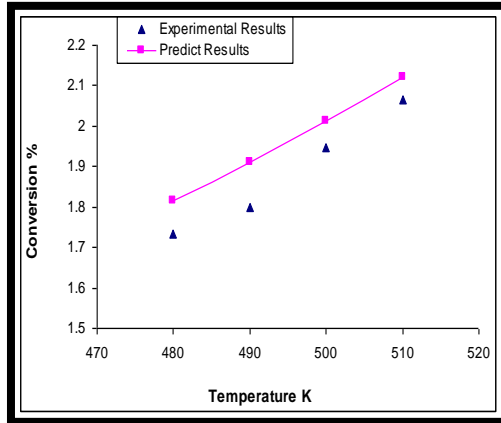
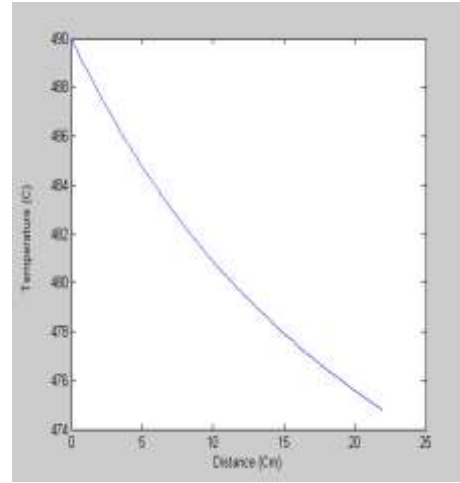
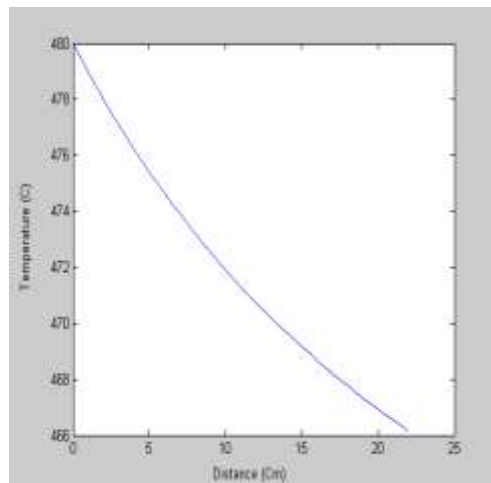


Figure (27) The comparison between the experimental and predicted aromatics conversion at WHSV (1hr<sup>-1</sup>) for (Pt-Sn / γ-Al<sub>2</sub>O<sub>3</sub>) catalyst.

Figure (28) The comparison between the experimental and predicted aromatics conversion at WHSV of (1hr<sup>-1</sup>) for (Pt-Ir / γ-Al<sub>2</sub>O<sub>3</sub>) catalyst.



**Figure (29)** Simulation of temperature profile for (Pt-Sn /  $\gamma$ -Al<sub>2</sub>O<sub>3</sub>) catalyst at 480 °C and (1hr<sup>-1</sup>). **Figure (30)** Simulation of temperature profile for (Pt-Sn /  $\gamma$ -Al<sub>2</sub>O<sub>3</sub>) catalyst at 490 °C and (1hr<sup>-1</sup>).

## CONCLUSIONS

The addition of tin (Sn) and iridium (Ir) to Pt/  $\gamma$ -Al<sub>2</sub>O<sub>3</sub> as bi-metal (Pt-Sn/ Al<sub>2</sub>O<sub>3</sub>, and Pt-Ir/Al<sub>2</sub>O<sub>3</sub>) improves the conversion of heavy naphtha reactants (Paraffins and Naphthenes). On the other hand, the selectivity of catalysts toward aromatization reactions especially light aromatics (A<sub>6</sub>, and A<sub>7</sub>) is increased.

The conversion of heavy naphtha reactants (Paraffins and Naphthenes) increases with increasing of reaction temperature in the range (480 – 510) °C. For the (Pt-Sn/ Al<sub>2</sub>O<sub>3</sub>) catalyst, the % conversion increasing from (14.75 % - 24.24 %) for (Paraffins), and (60 % - 71.9 %) for (Naphthenes), while, for the (Pt-Ir/ Al<sub>2</sub>O<sub>3</sub>) catalyst the % conversion increasing from (8.57 % - 16.7 %) for (Paraffins) and (50 % - 63.15 %) for (Naphthenes) and decreases with increasing of weight hour space velocity above (1 hr<sup>-1</sup>). The yield of the desired products (Aromatics) increases with increasing of reaction temperature in the range (480 – 510) °C. It was concluded that for (Pt-Sn/ Al<sub>2</sub>O<sub>3</sub>) catalyst increasing from (28.27 % - 33.67 %), while for (Pt-Ir/ Al<sub>2</sub>O<sub>3</sub>) catalyst increasing from (24.51% - 29.41%) and decreases with increasing of weight hour space velocity.

The derived model and simulation agrees with the experimental work results according to the suggested scheme of reactions network for heavy naphtha reforming. And the comparison of the model results with experimental results shows a deviation range of 1.93% to 14.51%.

## REFERENCES

- [1]. Silvana, A.D., Carlos R.V., Florence E., Catherine E., Patrice M., Carlos L.P., "Naphtha Reforming Pt-Re-Ge/  $\gamma$ -Al<sub>2</sub>O<sub>3</sub> Catalysts Prepared by Catalytic Reduction (Influence of the pH of the Ge Addition Step)", J. Catal Today, vol. 133-135, p 13-19, (2008).
- [2]. Shahrazad, R. Raouf, Moayed G. Jalhoom, Ramzy S. Hamied, "Preparation and Catalytic Study of Selected Types of ZSM5-Zeolites" Eng. &Tech. Journal, vol.29, No.13, (2011).
- [3]. Meyers, R.A., "HandBook of Petroleum Refining Processing", McGraw Hill, 3<sup>rd</sup> Edition, Copyrighted Material, USA, (2006).
- [4]. Gholamreza, Z., Tarin M., Biglari M., " Dynamic Modeling and Simulation of Industrial Naphtha Reforming Reactor", World Academy of Sci., Eng. and Technology, vol. 67, p 911, (2012).

- [5]. Aboalfazl, A., Hajir K., Reza M., Mehdi G., "Simulation and Modeling of Catalytic Reforming Process", *Petroleum & Coal*, vol. 54 (1), p 76-84, (2012).
- [6]. Carvalho, L.S., Piek C.L., Rangel M.C., Figoli N.S., Grau J.M., Reyes P., Parera J.m., "Trimetallic Naphtha Reforming Catalysts. I. Prop. of the Metal Funct. and Influence of the Order of Addition of the Metal Precursors on Pt-Re-Sn/  $\gamma$ -Al<sub>2</sub>O<sub>3</sub>-Cl", *J. Appl. Catal. A*: vol. 269, p 91-103, (2004).
- [7]. Weifeng, H., Hongye S., Yongyou H., and Tiom C., "Modeling, Simulation and Optimization of a whole Industrial Catalytic Naphtha Reforming Process on Aspen plus Platform", *Chinese, J. Chem. Eng.*, vol. 14, No 5, p 584, (2006).
- [8]. Khalid, A. Sukkar, Hayam M. Abdal-Raheem, Amel Th. Juber, and Jabir Sh. Jumaly, "Study of Catalysts Deactivation in Isomerization Process to produce High Octane Gasoline" *Iraqi J. of Chem. and Petrol. Eng.*, vol.8, No.3, p 43-48, Sept., (2007).
- [9]. González, M.P., Iñarra B., Guil J.M., Gutiérrez M.A., "Development of an Industrial Characterization Method for Naphtha Reforming Bimetallic Pt-Sn/ $\gamma$ -Al<sub>2</sub>O<sub>3</sub> Catalysts through n-heptane Reforming Test Reaction", *J. Catal. Today*, vol. 107-108, p 685-692, (2005).
- [10]. Fogler, S.C., "Element of Chem. React. Eng.", 2<sup>nd</sup> Edi., Prentice-Hall of India Private Limit., (1997).
- [11]. Yong, H., Hongy S., Jian C., " Modeling, Simulation and Optimization of Commercial Naphtha Catalytic Reforming Process ", *Proceeding of the 42<sup>nd</sup> IEEE Conf, USA, (Dec)*, p 6206, (2003).
- [12]. Aguilar, R.E., Ancheyta J.J., " New Process Model Proves Accurate in Tests on Catalytic Reformer", *Oil Gas J.*, vol. 25, p 80-83, (1994).
- [13]. Gates, B.C., Katzer J.R., Schuilt G.C.A., " Chemistry of Catalytic Processes", McGraw-Hill book Co. New York, p 184, (1979).
- [14]. Villafertre, E., Jorge A.J., " Kinetic and Reactor Modeling of Naphtha Reforming Process", *J. Petroleum and Coal*, vol. 44, 1-2, p 63-66, (2002).
- [15]. Lu, H., " Manual of Petrochem. Indu. Fund. Data", Chem. Indu. Press, Beijing, China, (1982).
- [16]. Seif Mohaddecy S.R., Zahedi S., Sadighi S., Bonyad H. 2006, " Reactor Modeling and Simulation of Catalytic Reforming Process ", *J. Petroleum and Coal*, vol 48, No3, p 28-35.
- [17]. Vanina, A.M., Javier M.G., Carlos R.V., Juan C.Y., José M.P., Carlos C.Y. 2005, " Role of Sn in Pt-Re-Sn/AL<sub>2</sub>O<sub>3</sub>-Cl Catalysts for Naphtha Reforming ", *J. Catal Today*, vol 107-108, p 643-650.
- [18]. Bednarova, L., Lyman C.E., Rytter E., Holmen A., *J. Catal*, vol. 211, p 335, (2002).
- [19]. Mohammed, A.A., Hussein K.H., " Catalytic Aromatization of Naphtha Using Different Catalysts", *Iraq. J. Chem. and Petr. Eng.*, vol. 5, (Dec), p 13, (2004).
- [20]. Jenkins, J.H., Stephens T.W. 1980, " Kinetics of Catalytic Reforming", *J. Hyd. Proc*, Nov, p 163-167.

- [21]. Ali, S.A., Siddiqui M.A.,” Parametric Study of Catalytic Reforming Process”,  
J. React. Kinet. Catal. Litt., vol. 87, (No 1), p 199-206, (2006).